Available online at www.sciencedirect.com

ScienceDirect

ELSEVIER

Ceramics International 34 (2008) 89–94

CERAMICS INTERNATIONAL

www.elsevier.com/locate/ceramint

TiO_2 as a sintering additive for $KNbO_3$ ceramics

Darko Makovec, Irena Pribošič [*], Miha Drofenik

"Jožef Stefan" Institute, Jamova 39, SI-1000 Ljubljana, Slovenia

Received 17 May 2006; received in revised form 9 August 2006; accepted 21 August 2006
Available online 13 October 2006

Abstract

Improved densification during the conventional sintering of $KNbO_3$ ceramics was achieved by using small additions of TiO_2. This improved densification can be explained on the basis of high-temperature chemical reactions in the system. X-ray diffractometry and electron microscopy were used in combination with diffusion-couple experiments in order to elucidate the chemical reactions between $KNbO_3$ and TiO_2. TiO_2 reacts with $KNbO_3$ forming $KNbTiO_5$, and a low concentration of Ti incorporates in the $KNbO_3$ structure resulting in the formation of oxygen vacancies and, consequently, in an improvement in the densification. At ~1037 °C eutectic melting between the $KNbO_3$ and the $KNbTiO_5$ further improves the densification of the $KNbO_3$ ceramics.

Keywords: A. Sintering; D. Niobates; D. TiO_2; $KNbO_3$

1. Introduction

Lead-containing perovskite ceramic materials, such as $PbTiO_3$, $(Ba,Pb)TiO_3$, $Pb(Zr,Ti)O_3$ or $Pb(Mg,Nb)O_3$, are industrially important, because of their high-temperature ferroelectricity, piezoelectricity and piroelectricity. However, since they contain poisonous lead, replacing them with lead-free ferroelectrics is a priority concern. $KNbO_3$-based ceramics – especially the solid solution of ferroelectric $KNbO_3$ (KN) and antiferroelectric $NaNbO_3$ (NN) with the composition $K_{0.5}Na_{0.5}NbO_3$ (KNN) – are potential materials for the replacement of lead-containing ferroelectrics. In 2004, Saito et al. [1] reported on the preparation of high-performance lead-free piezoceramics based on KNN. Using a combination of appropriate additives and a processing route they produced highly $\langle 0\,0\,1 \rangle$ textured ceramics and an electric-field-induced strain comparable to a typical actuator-grade PZT [1]. Ceramics based on KN were also tested as lead-free materials with a positive temperature coefficient of resistivity (PTCR) [2–4]. Moreover, KN is also one of the most promising materials for nonlinear optical and electro-optical devices because of its large nonlinear susceptibility and high photorefractive coefficient [5].

The main problem in the commercialization of $KNbO_3$-based ceramics for various applications is related to the sintering. Classical pressureless sintering of $KNbO_3$ or of $K_{0.5}Na_{0.5}NbO_3$ is technically difficult due to the large differences in the properties of the cations involved. There is also the problem of stoichiometry control and densification during long-term sintering because of the rapid vaporization of K_2O. In order to improve the sinterability of $KNbO_3$, different additives have been used [6–11]. Kosec and Kolar [6], for example, used additions of MgO to improve the densification of $KNaNbO_3$. Mg^{2+} presumably incorporated into the $KNaNbO_3$ structure causing the formation of lattice defects; this increased the lattice diffusion and, consequently, improved the densification. Ahn and Schulze [7] reported an increase in the densification of $KNaNbO_3$ with the addition of BaO. Tashiro et al. [8] reported improvements in the sinterability of $KNbO_3$ by substituting a small amount of Pb for K. The improved sinterability was explained by the presence of a liquid phase. Improvements of the sinterability of $KNbO_3$ ceramics with an addition of PbO were also reported by Pribošič et al. [3]. Some additives, like $LaFeO_3$ [9], $SrTiO_3$ [10] or $BaTiO_3$ [4,11], which form perovskite solid solutions with $K(Na)NbO_3$ were also reported to improve the densification of $KNbO_3$.

In this work, we report on the microstructure and an improved densification of $KNbO_3$ ceramics with small additions of TiO_2. The reasons for the improved densification

---

[*] Corresponding author. Tel.: +386 14773895; fax: +386 14773171.
E-mail address: irena.pribosic@ijs.si (I. Pribošič).

0272-8842/$32.00 © 2006 Elsevier Ltd and Techna Group S.r.l. All rights reserved.
doi:10.1016/j.ceramint.2006.08.008

are discussed on the basis of the high-temperature reactions studied in the system.

2. Experimental

$KNbO_3$ powder was prepared by calcinating of stoichiometric quantities of K_2CO_3 (Alfa, 012609) and Nb_2O_5 (Alfa, 011366) at 830 °C for 12 h. The potassium carbonate was dried at 200 °C for 2 h before use. The calcined material was milled for 4 h in ethanol using an attritor mill with zirconia balls. The X-ray diffractogram (XRD) of the $KNbO_3$ powder only showed peaks corresponding to orthorhombic $KNbO_3$. The prepared $KNbO_3$ powder was mixed with different additions (2, 10, 20, 50, 66, 75, and 87 mol.%) of TiO_2 (Bayer, T) by ball milling in ethanol for 2 h. The powders were granulated with the use of camphor and then uniaxially pressed into tablets, 6 mm in diameter and approximately 6 mm high, with a pressure of ~150 MPa. The tablets were sintered for 2 h at different temperatures in air. The samples were characterized using XRD (Model D4 Endeavor, Bruker AXS, Karlsruhe, Germany), scanning electron microscopy (SEM) (JEOL 4800 with a LINK ISIS EDS 300 Analyser) and transmission electron microscopy (TEM) (JEOL, JEM 2010 F). Quantification of the EDS spectra was performed with Oxford ISIS software using a library of virtual standards.

The specimens for the TEM were prepared by cutting 3-mm diameter discs from the ceramic bodies. These discs were reduced to ~120 μm by grinding. A region about 20-μm thick at the centre of the disc was produced using a dimple grinder. Finally, the specimens were thinned by argon-ion erosion at 4 kV with an incident angle of about 10°.

The densities of the samples were measured picnometrically, by immersing them into Hg. The shrinking of the samples during sintering was followed with a computerized heating microscope. The heating rate was 5 °C/min. The melting temperatures of the different compositions were estimated from the shrinkage curves.

The chemical reactions, which occurred between pre-calcined $KNbO_3$ powder and TiO_2 at high temperatures, were also studied using diffusion-couple experiments. For the purpose of constructing the diffusion couples, the $KNbO_3$ powder was pressed into a pellet with a diameter and height of 3 mm. The $KNbO_3$ tablet was subsequently embedded into the TiO_2 powder and pressed into a pellet with a diameter and height of 12 mm. After sintering at different temperatures, the diffusion couples were cut parallel to the pressing direction. The interface between the two materials was studied using SEM.

3. Results

3.1. Chemical reactions in the $KNbO_3$–TiO_2 quasi-binary system

The $KNbO_3$–TiO_2 diffusion couple, prepared by heating at 1050 °C – the temperature that is normally used for sintering $KNbO_3$ ceramics – cracked at the interface in spite of intensive interface chemical reactions between the two components. The interface cracking is a consequence of the much faster shrinking of the TiO_2 compared to that of the $KNbO_3$ during heating. However, it was clear that the $KNbO_3$ part of the diffusion couple was partially melted. This melting of the $KNbO_3$ could be associated with the appearance of a eutectic liquid phase between the $KNbO_3$ and one of the phases, formed by the reaction between the two components.

Fig. 1 shows a cross-section (SEM–BSI) of the $KNbO_3$–TiO_2 diffusion couple, heated for 2 h at 1060 °C. In this case, all the $KNbO_3$ reacted with the TiO_2 and a sequence of products was formed. The composition of the products was measured using EDS analysis. In contact with TiO_2 is a layer of the compound $K_2Ti_6O_{13}$. This layer is followed by a thin layer of the compound $KNbTi_3O_9$. The following layer is composed of large crystals of the compound $KNbTiO_5$, elongated in the direction of growth (perpendicular to the original interface between the two starting components). The compact layer of $KNbTiO_5$ extends into the porous two-phase region in the vicinity of a large crack. This two-phase region is composed of elongated crystals of $KNbTiO_5$ and of the Nb-rich compound $K_4Nb_6O_{17}$.

The sequence of products formed in the diffusion couple between the TiO_2 and $KNbO_3$ is a consequence of the counter-diffusion of the ions that have very different diffusivities. The reactions occur by the migration of potassium and niobium towards the TiO_2. The K- and Nb-rich part is thus very porous (Kirkendall porosity) [12]. In the part of the diffusion couple shown in Fig. 1, the pores are segregated in the form of a crack that extends parallel to the original interface between the two components. Potassium diffuses much faster than niobium, resulting in the formation of the compound $K_2Ti_6O_{13}$ in the contact with the TiO_2 and the formation of the compound $K_4Nb_6O_{17}$ at the $KNbO_3$ part of the diffusion couple. Two ternary compounds are formed in the middle of the reaction layer as a consequence of reactions between the oxides of potassium, niobium and titanium, i.e., $KNbTi_3O_9$ and $KNbTiO_5$.

The formation of the compounds $KNbTi_3O_9$ and $KNbTiO_5$ from the reaction between $KNbO_3$ and TiO_2 is in agreement

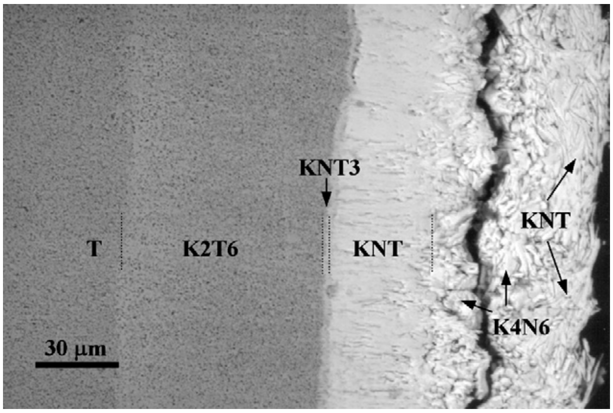

Fig. 1. Cross-section (SEM–BSI) of the $KNbO_3$–TiO_2 diffusion couple heated for 2 h at 1080 °C (T: TiO_2, K2T6: $K_2Ti_6O_{13}$, KNT3: $KNbTi_3O_9$, KNT: $KNbTiO_5$, K4N6: $K_4Nb_6O_{17}$).

with the results obtained with the XRD analysis of the samples that were prepared by heating different intimate mixtures of $KNbO_3$ and TiO_2 at 1035 °C (Fig. 2). The analysis of the samples with different compositions proved that only those two compounds are stable in the $KNbO_3$–TiO_2 quasi-binary system.

The melting temperatures of the samples were determined with a heating microscope. The melting temperature of pure $KNbO_3$ was determined to be approximately 1060 °C. The addition of up to 50 mol.% TiO_2 decreased the melting temperature of $KNbO_3$: melting of the $KNbO_3$ samples containing up to 50 mol.% TiO_2 was detected at 1037 °C. These results could be explained by a eutectic between the $KNbO_3$ and the $KNbTiO_5$. However, the appearance of the melt could also be a consequence of the differences in the diffusivities of the involved ions. The analyses of the diffusion couples showed that $KNbO_3$ degrades in the contact with TiO_2. Due to a much faster diffusion of K^{1+} compared to Nb^{5+}, the transient liquid phase originating from the K_2O-rich part of the K_2O–Nb_2O_5 system [13,14] or from the K_2O–TiO_2 system [15] could form in the contact with TiO_2.

Melting of the composition 50 mol.% $KNbO_3$–50 mol.% TiO_2, corresponding to the compound $KNbTiO_5$, was detected at approximately 1150 °C, while the composition 25 mol.% $KNbO_3$–75 mol.% TiO_2, corresponding to the compound $KNbTi_3O_9$, melted above 1300 °C.

3.2. Sintering and microstructure of $KNbO_3$ ceramics with a small addition of TiO_2

Fig. 3 shows XRD spectra of the $KNbO_3$ samples with different additions of TiO_2, sintered for 2 h at 1030 °C. The XRD spectrum of the undoped $KNbO_3$ consists of sharp peaks that correspond to the orthorhombic perovskite structure. Already with the addition of 0.5 mol.% TiO_2, the peaks become broader, while a number of distinct peaks due to orthorhombic distortion merged into a single peak. The merging of the orthorhombic peaks into one broad, asymmetric peak suggests an increase in the symmetry of the crystal structure. At the same time, the peaks are broadened due to internal stress and the small grain size in the $KNbO_3$ samples with small additions of TiO_2. The microstructure of the samples is explained later in the text. With the addition of 2 mol.% TiO_2 to the $KNbO_3$, small peaks corresponding to the secondary phase $KNbTiO_5$ appeared in the XRD spectrum (Fig. 3).

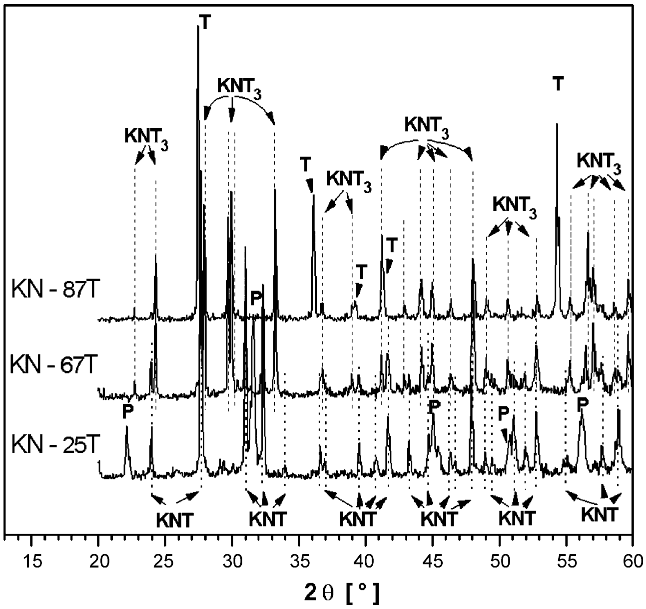

Fig. 2. XRD spectra of different compositions from the $KNbO_3$–TiO_2 quasi-binary system. KN-25T: 75 mol.% $KNbO_3$–25 mol.% TiO_2; KN-67T: 33 mol.% $KNbO_3$–67 mol.% TiO_2; KN-87T: 13 mol.% $KNbO_3$–87 mol.% TiO_2. The intimate mixtures of $KNbO_3$ and TiO_2 were heated for 4 h at 1030 °C (P: $KNbO_3$ perovskite, KNT: $KNbTiO_5$, KNT_3: $KNbTi_3O_9$, T: TiO_2 rutile).

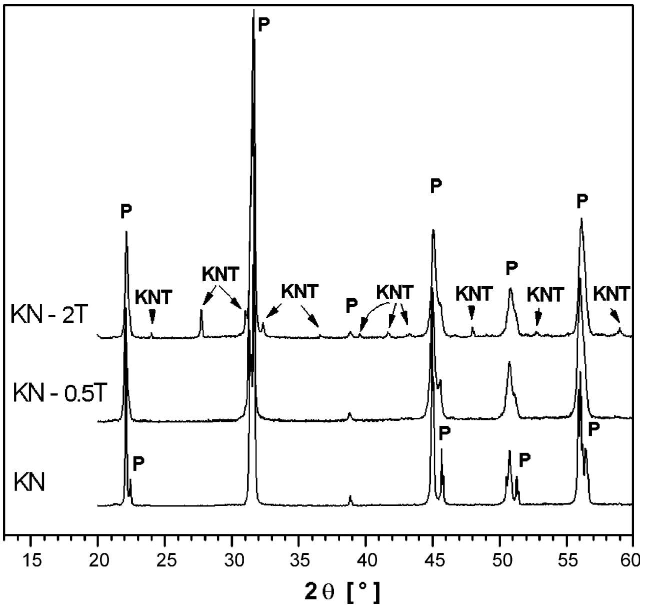

Fig. 3. XRD spectra of the $KNbO_3$ samples with the addition of different amounts of TiO_2. KN: $KNbO_3$ without the addition of TiO_2; KN-0.5T: $KNbO_3$ with the addition of 0.5 mol.% of TiO_2; KN-2T: $KNbO_3$ with the addition of 2 mol.% of TiO_2. The samples were prepared by sintering for 2 h at 1030 °C (P: $KNbO_3$ perovskite, KNT: $KNbTiO_5$).

The changes in the structure of the $KNbO_3$ with the addition of TiO_2 detected by XRD strongly suggest that some of the Ti incorporates into the $KNbO_3$ perovskite structure. The results are in accordance with the work of Sundarakannan et al. [16], who concluded on the basis of Raman spectroscopy and measurements of the dielectric properties of $KNbO_3$ with different additions of TiO_2, that a low concentration of Ti enters the $KNbO_3$ perovskite structure substitutionally at the octahedrally coordinated Nb lattice sites. The temperature of the permittivity maximum of the $KNb_{1-X}Ti_XO_{3-X/2}$ compositions decreased significantly for $X = 0.002$, while a further increase in the Ti content had only a minor effect on the temperature of the permittivity maximum [16].

The addition of a small amount of TiO_2 has a remarkable influence on the densification and microstructure development of $KNbO_3$ ceramics. The undoped $KNbO_3$ sample sintered for 2 h at 1050 °C was relatively porous, having a density of approximately 92% of theoretical density (TD = 4.617 g/cm^3). With the addition of 0.5 mol.% of TiO_2, the density of the

$KNbO_3$ sample sintered for 2 h at 1050 °C increased to 96% TD. The samples containing larger additions of TiO_2 (2 mol.% TiO_2 and 4 mol.% TiO_2) were partially melted at 1050 °C. A temperature of 1040 °C was determined to be the optimum sintering temperature for those samples. The densities of the samples sintered for 2 h at 1040 °C were 86% TD, 92% TD, 95% TD and 96% TD for additions of 0, 0.5, 2 and 4 mol.% TiO_2, respectively.

The shrinkage of the samples during sintering was followed using a heating microscope. Fig. 4 shows a comparison of the shrinkage and the shrinkage-rate spectra for the undoped $KNbO_3$ and the $KNbO_3$ with the addition of 2 mol.% TiO_2. The $KNbO_3$ sample without the additive shrank with a very slow rate up to a temperature of approximately 1045 °C. At this temperature, only ~15 °C below the melting point, the shrinkage rate abruptly increased and reached ~1% min^{-1} at ~1055 °C. The $KNbO_3$ sample with the addition of TiO_2 started to shrink with a slightly lower rate than the undoped sample; however, at around 1000 °C the shrinkage rate increased sharply. At temperatures above ~1030 °C, the slope of the shrinkage curve further increased and the shrinkage rate reached ~2.7% min^{-1}, and its maximum at ~1045 °C. The final shrinkage of the $KNbO_3$ sample with and without the addition of TiO_2 was 17 and 14%, respectively.

The addition of TiO_2 also had a large effect on the microstructure of the $KNbO_3$ ceramics. The microstructure of the $KNbO_3$ without the addition of TiO_2 was fine grained, with an average grain size of approximately 2.5 μm, as can be seen on the fracture surface (Fig. 5(a)). The addition of TiO_2 to $KNbO_3$ dramatically decreased the grain size. Thus, in the samples with the addition of 0.5–4 mol.% TiO_2 the grain size was below 0.5 μm (Fig. 5(b)).

The TEM analysis of the $KNbO_3$ sample with the addition of 2 mol.% TiO_2, which was sintered for 2 h at 1020 °C, showed a homogeneous, fine-grained microstructure. In between the $KNbO_3$ matrix grains, smaller individual plate-like grains of the $KNbTiO_5$ compound were present. However, no amorphous phase could be detected at the grain boundaries using HREM imaging (Fig. 6). The EDS analysis of the matrix grains showed the presence of only K, Nb and O, while Ti could not be detected. The detection limit of the EDS analysis for the Ti in the matrix of $KNbO_3$ was estimated to be below 0.8 mol.%. The

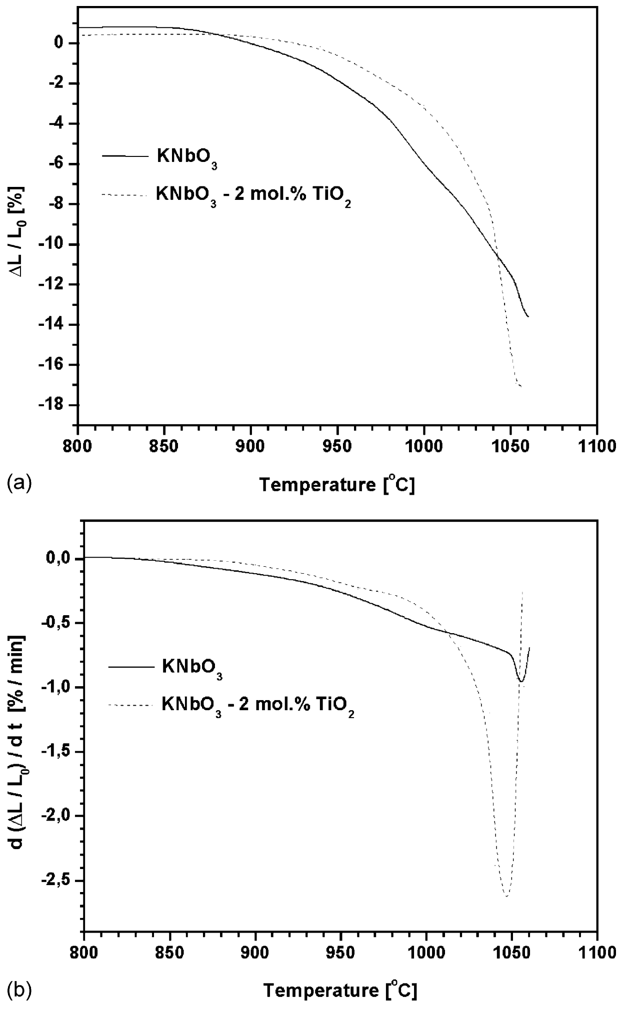

Fig. 4. Comparison of shrinkage curves (a) and corresponding shrinkage-rate spectra (b) for undoped $KNbO_3$ and $KNbO_3$ with the addition of 2 mol.% TiO_2 (heating rate 5 °C/min).

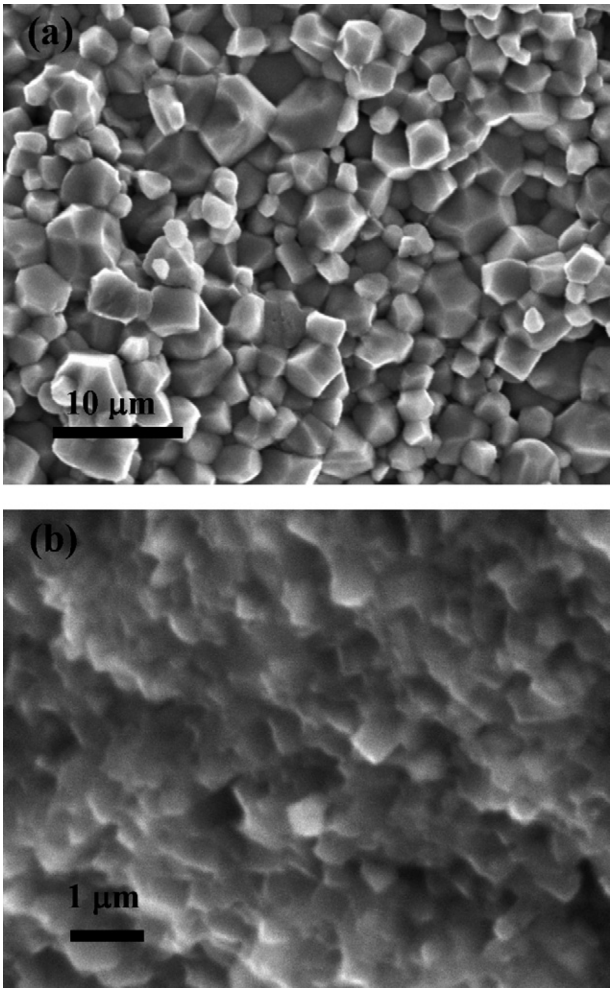

Fig. 5. The microstructure of $KNbO_3$ (a) and $KNbO_3$ with the addition of 2 mol.% TiO_2 (b), both sintered for 2 h at 1050 °C.

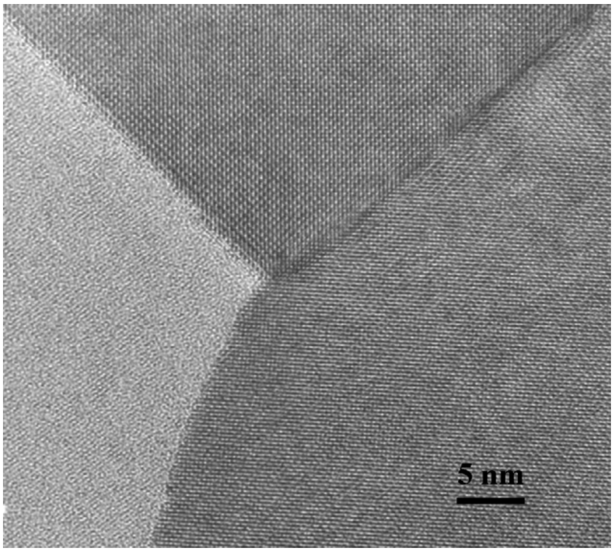

Fig. 6. HREM image of the triple point between the $KNbO_3$ grains in the $KNbO_3$ sample with the addition of 2 mol.% TiO_2, sintered for 2 h at 1020 °C.

result shows that the solubility of TiO_2 in the matrix grains is very low. However, the EDS analysis of the grain boundaries usually revealed a low content of Ti, suggesting the segregation of Ti at the grain boundaries.

When the sample was sintered for 2 h at 1040 °C, the triple points between the matrix grains were frequently filled with pockets of solidified liquid phase. Rarely, small plate-like crystallites of the secondary phase were present at the triple points, as shown in Fig. 7(a). The EDX analysis of the region with the crystallites showed a high content of Ti (in addition to K, Nb and O), whereas the electron diffraction patterns taken from the region with the precipitate matched the structure of the orthorhombic compound $KNbTiO_5$ (Fig. 7(b)).

4. Discussion

The addition of small amounts of TiO_2 effectively improved the densification of $KNbO_3$. At temperatures around 1000 °C, the $KNbO_3$ with the addition of TiO_2 started to densify much faster than the pure $KNbO_3$. The increase in the densification rate of the sample with the TiO_2 addition suddenly further increased at around 1040 °C (Fig. 3).

The increase in the densification rate due to the minor additive could be explained: (i) by the appearance of a reactive liquid phase in the system, or (ii) by a change in the lattice diffusion due to the formation of lattice defects related to the additive incorporation into the matrix phase.

The TEM analysis showed that at the grain boundaries and the triple points of the $KNbO_3$ sample sintered at 1040 °C with the addition of 2 mol.% TiO_2, the remnants of the Ti-rich liquid phase are present. Melting of the $KNbO_3$ with an addition of up to 50% TiO_2 was observed at temperatures around 1037 °C; this is approximately 23 °C below the observed melting temperature of pure $KNbO_3$. The melting of these compositions is a consequence of the eutectic between the $KNbO_3$ and the $KNbTiO_5$ ternary compound, which is formed by the reaction between TiO_2 and $KNbO_3$. The $KNbTiO_5$ compound was already detected in the starting powder, which was prepared by calcination for 12 h at 830 °C. The appearance of the eutectic melt coincides with the sudden increase in the densification rate observed during the sintering of the $KNbO_3$ with the addition of 2 mol.% TiO_2 at approximately 1040 °C. Thus, the increase in the sintering rate above 1040 °C could be ascribed to the appearance of the eutectic liquid phase.

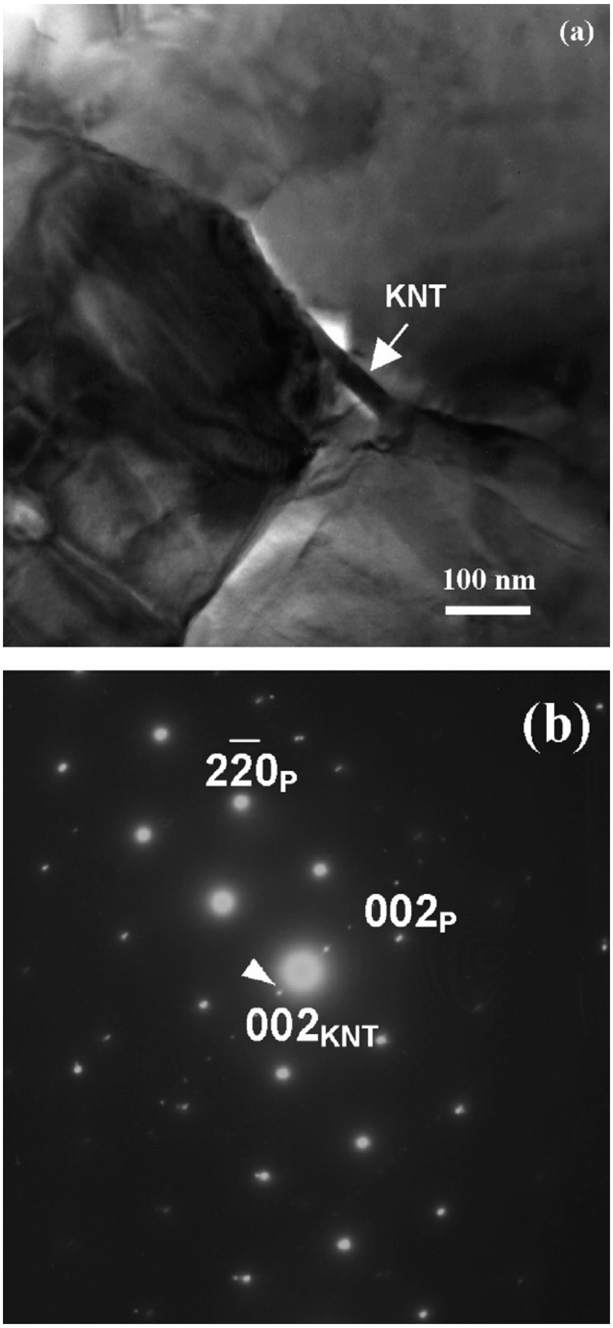

Fig. 7. (a) TEM BF image of the triple point between the $KNbO_3$ grains in the $KNbO_3$ sample with the addition of 2 mol.% TiO_2, sintered for 2 h at 1040 °C. The plate-like crystallite of $KNbTiO_5$ (KNT) is marked with an arrow. (b) Electron diffraction pattern taken from the area of the sample with the $KNbO_3$ perovskite grain (P) shown at the left-hand side of the BF image (Fig. 7(a)), and the triple point with the plate-like crystallite of $KNbTiO_5$ (KNT).

The addition of the TiO_2 to the $KNbO_3$ already increased the densification rate at approximately 1000 °C, i.e., much below the temperature of the eutectic between $KNbO_3$ and $KNbTiO_5$. As suggested by the diffusion-couple experiments, the transient liquid phase could locally appear in the system even at temperatures below that of the $KNbO_3$–$KNbTiO_5$ eutectic due to the very different diffusivities of the cations involved in the reaction between the $KNbO_3$ and TiO_2. However, no remnants of such a liquid phase could be detected at the grain boundaries and the triple points of the samples sintered below the $KNbO_3$–$KNbTiO_5$ eutectic temperature using HREM. Thus, it is most likely that at temperatures below that of the $KNbO_3$–$KNbTiO_5$ eutectic the addition of TiO_2 increases the densification of $KNbO_3$ by changing the lattice diffusion in the matrix phase. The incorporation of Ti^{4+} into the $KNbO_3$ structure as an acceptor at the Nb^{5+} lattice sites [14] results in the formation of the ionized oxygen vacancies as compensation defects maintaining the overall electroneutrality of the solid solution ($KNb_{1-X}Ti'_XO_{3-X/2}(V^{\bullet\bullet}{}_O)_{X/2}$). The increase in the oxygen-vacancy concentration in the $KNbO_3$ increases the oxygen lattice diffusion in the system and might significantly improve the densification of the ceramics [6,17].

5. Conclusions

Small additions of TiO_2 improve the densification of $KNbO_3$ ceramics and suppress the grain growth. The increase in the densification at temperatures above ∼1040 °C is explained by the appearance of the reactive liquid phase due to the eutectic between $KNbO_3$ and $KNbTiO_5$. Below the temperature of this eutectic, the enhancement in the densification by the addition of TiO_2 is attributed to an increase in the diffusion related to the formation of oxygen vacancies by the incorporation of the Ti_{Nb} acceptors into the $KNbO_3$ structure.

Acknowledgement

The support by the Ministry of Higher Education, Science and Technology of the Republic of Slovenia within the National Research Program is gratefully acknowledged.

References

[1] Y. Saito, H. Takao, T. Tani, T. Nonoyama, K. Takatori, T. Homma, T. Nagaya, M. Nakamura, Lead-free piezoceramics, Nature 432 (2004) 84–87.

[2] I.P. Raevnskii, E.I. Bondarenko, A.N. Pavlov, O.I. Prokopalo, PTCR effect in $KNbO_3$, Ferroelectrics 76 (1987) 55–60.

[3] I. Pribošič, D. Makovec, M. Drofenik, PTCR effect in Pb-doped $KNbO_3$, J. Mater. Res. 17 (12) (2002) 2989–2992.

[4] I. Pribošič, D. Makovec, M. Drofenik, Electrical properties of $KNbO_3$–$BaTiO_3$ ceramics, in: Proceedings of the Seventh Conference of the ECERS, 2001, pp. 1401–1404.

[5] D. Xue, S. Zhang, Linear and nonlinear optical properties of $KNbO_3$, Chem. Phys. Lett. 291 (1998) 401–406.

[6] M. Kosec, D. Kolar, On activated sintering and electrical properties of $NaKNbO_3$, Mater. Res. Bull. 10 (1975) 335–340.

[7] Z.S. Ahn, W.A. Shulze, Conventionally sintered $(Na_{0.5},K_{0.5})NbO_3$ with barium additions, J. Am. Ceram. Soc. 70 (1987), C-18-21.

[8] S. Tashiro, H. Nagamatsu, K. Nagata, Sinterability and piezoelectric properties of $KNbO_3$ ceramics after substituting Pb and Na for K, Jpn. J. Appl. Phys. 41 (2002) 7113–7118.

[9] K. Kakimoto, I. Masuda, H. Ohsato, Ferroelectric and piezoelectric properties of $KNbO_3$ ceramics containing small amounts of $LaFeO_3$, Jpn. J. Appl. Phys. 42 (2003) 6102–6105.

[10] Y.P. Guo, K. Kakimoto, H. Ohsato, Dielectric and piezoelectric properties of lead-free $(Na_{0.5}K_{0.5})NbO_3$–$SrTiO_3$ ceramics, Solid State Commun. 129 (2004) 279–284.

[11] Y.P. Guo, K. Kakimoto, H. Ohsato, Structure and electrical properties of lead-free $(Na_{0.5}K_{0.5})NbO_3$-$BaTiO_3$ ceramics, Jpn. J. Appl. Phys. 43 (9B) (2004) 6662–6666.

[12] A.D. Smigelskas, E.O. Kirkendall, Zinc diffusion in alpha brass, Trans. Am. Inst. Mechan. Eng. 171 (1947) 130–134.

[13] A. Reisman, F. Holzberg, Phase equilibria in the system K_2CO_3-Nb_2O_5 by the method of differential thermal analysis, J. Am. Chem. Soc. 77 (8) (1955) 2115–2119.

[14] E. Irle, R. Blatchnik, B. Gather, The phase diagrams of Na_2O and K_2O with Nb_2O_5 and the ternary system Nb_2O_5–Na_2O–Yb_2O_3, Thermochim. Acta 179 (1991) 157–169.

[15] G. Eriksson, A.D. Pelton, Critical-evaluation and optimization of the thermodynamic properties and phase-diagrams of the MnO–TiO_2, MgO–TiO_2, FeO–TiO_2, Ti_2O_3–TiO_2, Na_2O–TiO_2, and K_2O–TiO_2 systems, Metall. Trans. B 24B (5) (1993) 795–805.

[16] B. Sundakarannan, K. Kakimoto, H. Ohsato, Ti and V substitutions on the $KNbO_3$ ceramics: dielectric study, Ferroelectrics 302 (2004) 175–179.

[17] C.H. Lu, L.C. De Jonghe, Influence of Nd_2O_3 doping on the reaction process and sintering behavior of $BaCeO_3$ ceramics, J. Am. Ceram. Soc. 77 (10) (1994) 2523–2528.